

Anisotropic jet broadening and jet shape

John Terry

Director's postdoctoral fellow, Los Alamos National Laboratory



Ongoing work in collaboration with

Wei-yao Ke and Ivan Vitev

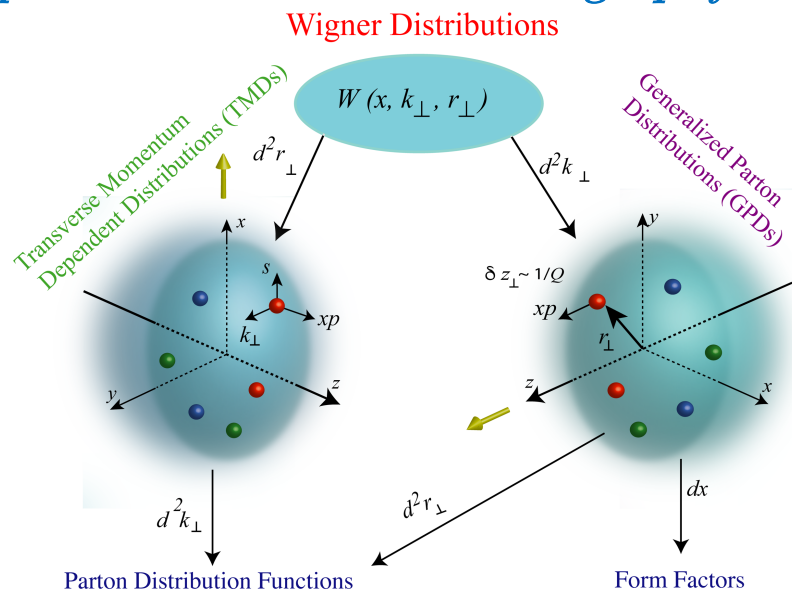
Heavy Ion Physics in the EIC Era
The Institute for Nuclear Theory
August 20



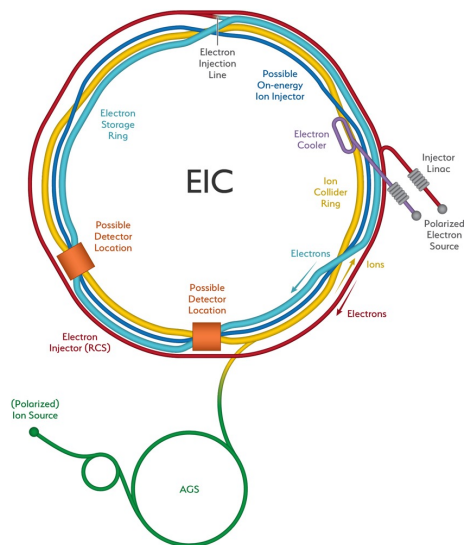
Background

Imaging hadronic structure and nuclear matter

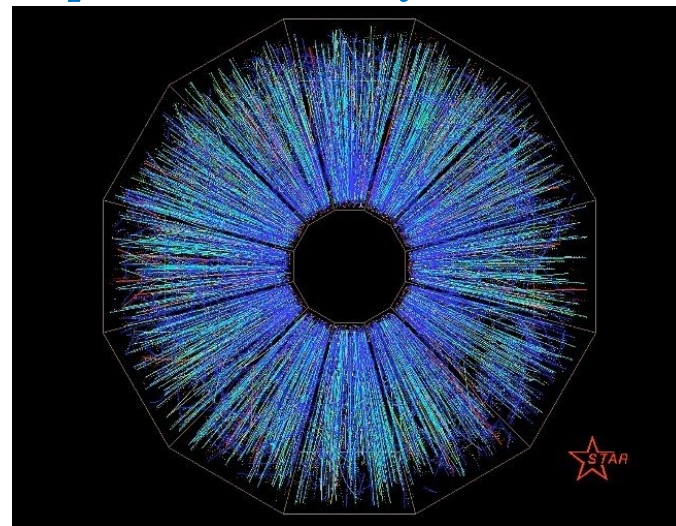
DIS experiments for hadron tomography



Jefferson Lab

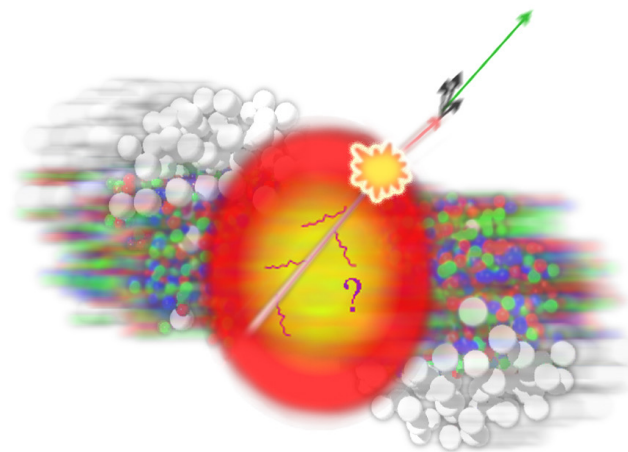


Heavy Ion experiments for QCD medium



$$\mathcal{L}_{\text{SCET}_G}(\xi_n, A_n, A_G) = \mathcal{L}_{\text{SCET}}(\xi_n, A_n) + \mathcal{L}_G(\xi_n, A_n, A_G),$$

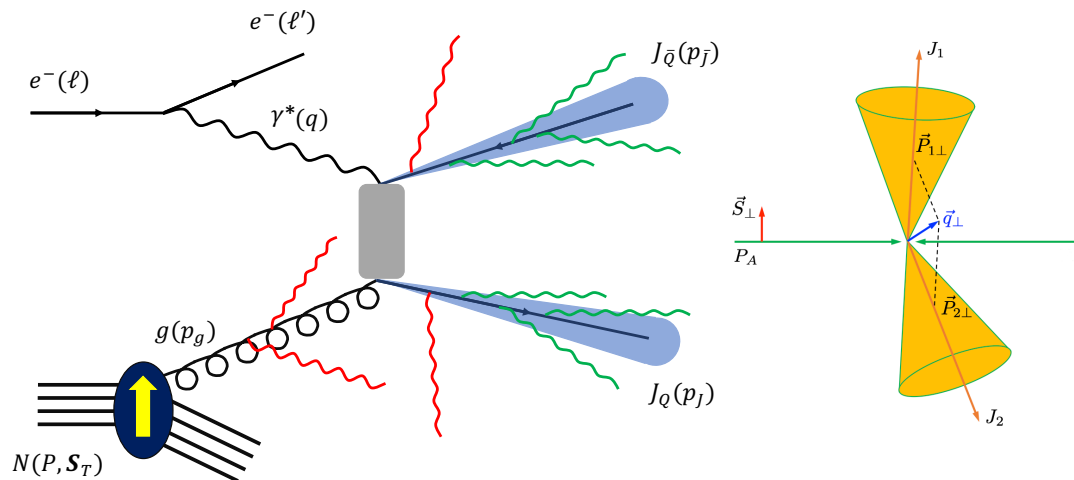
$$\mathcal{L}_G(\xi_n, A_n, A_G) = \sum_{p,p'} e^{-i(p-p')x} \left(\bar{\xi}_{n,p'} \Gamma_{\text{qqAG}}^{\mu,a} \frac{\not{n}}{2} \xi_{n,p} - i \Gamma_{\text{ggAG}}^{\mu\nu\lambda,abc} (A_{n,p'}^c)_\lambda (A_{n,p}^b)_\nu \right) A_{G\mu,a}(x)$$



How and why are jets useful?

Jets act as a clean proxy for the direction of the parent parton

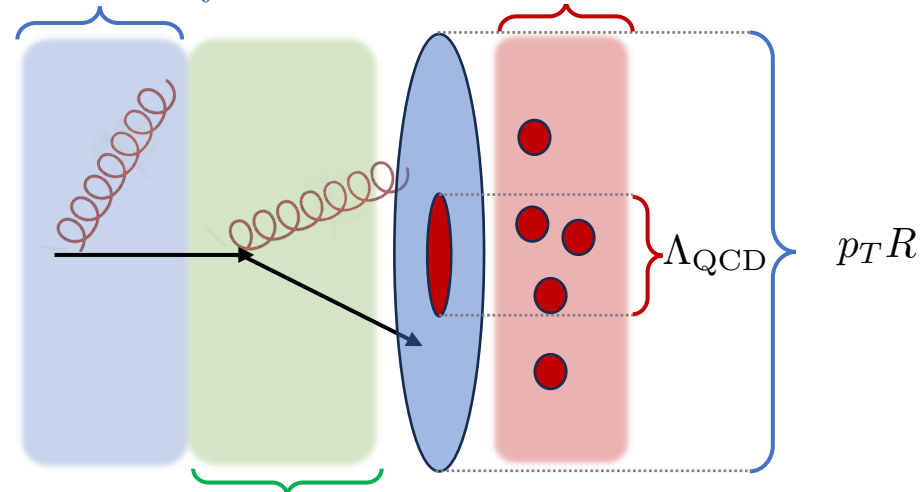
Di-jet decorrelations in ep



Anatomy of a jet

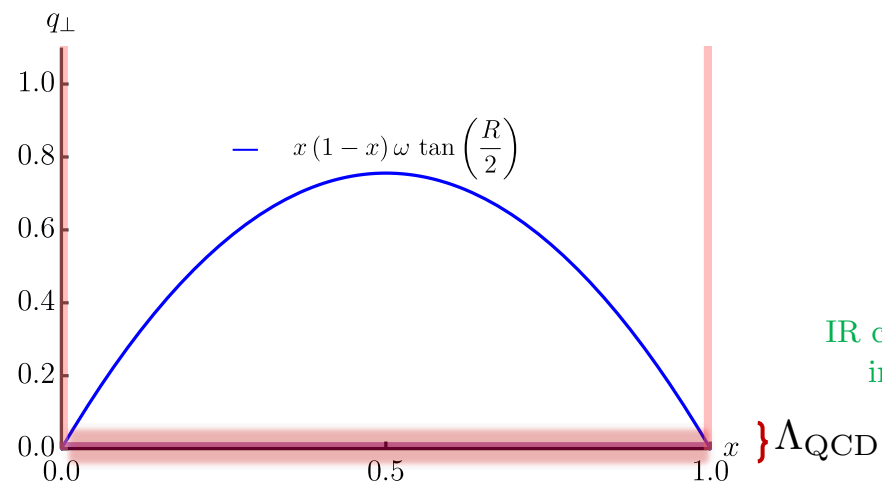
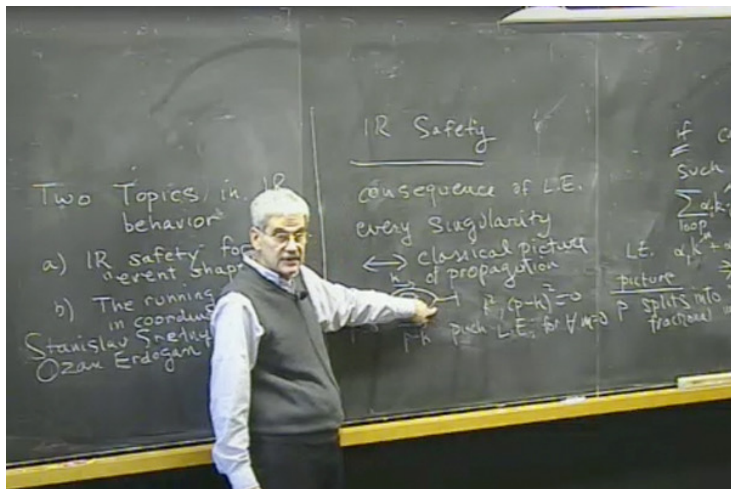
Perturbative correction to jet direction

Hadronization



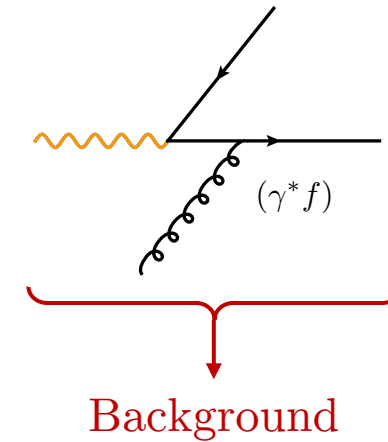
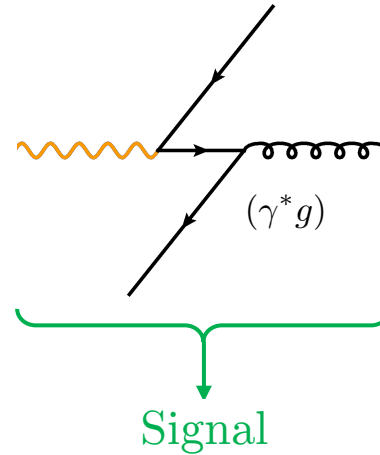
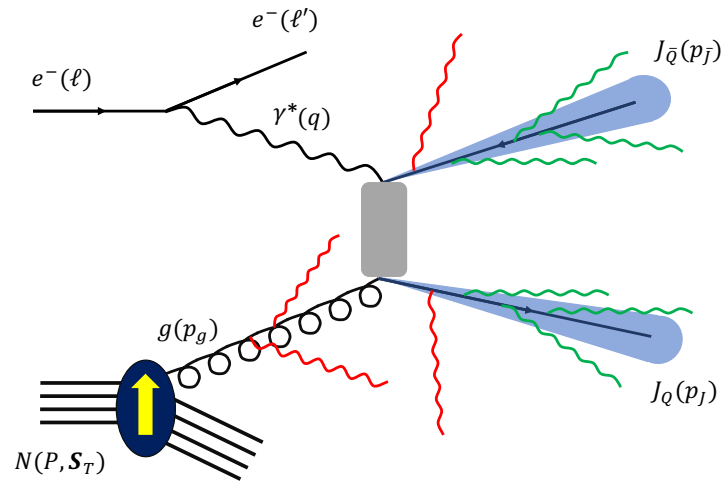
Perturbative correction to jet

Hadronization effects do not affect the direction of the jet in the limit that Sterman Weinberg 1977



Limitations of jets

Often physical processes contain background effects, jets are limited in their ability to limit this

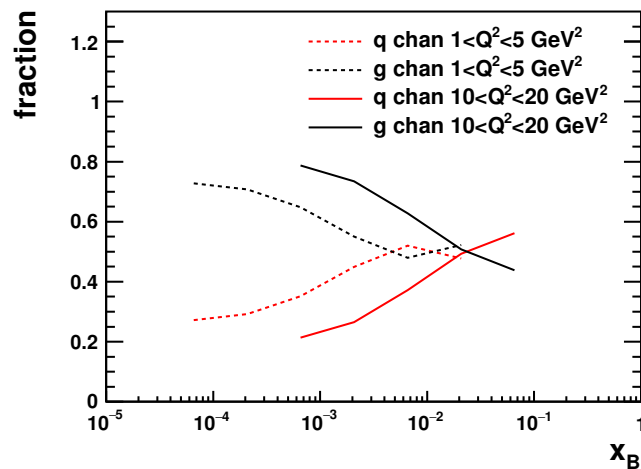


We can reduce the background kinematically, but this is not ideal

Castillo, Echevarria, Makris, Scimemi 2021

Kang, Reiten, Shao, Terry 2021

Zheng, Aschenauer, et al 2018

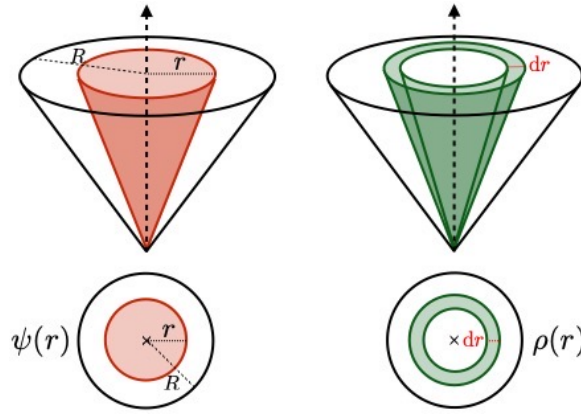


Accessing the gluon distributions at moderate to large x becomes difficult

Jet substructure observables

The pattern of radiation is correlated with the quantum numbers of the parent parton

Jet shape: Provides information for the energy of the jet as a function of the sub-jet radius



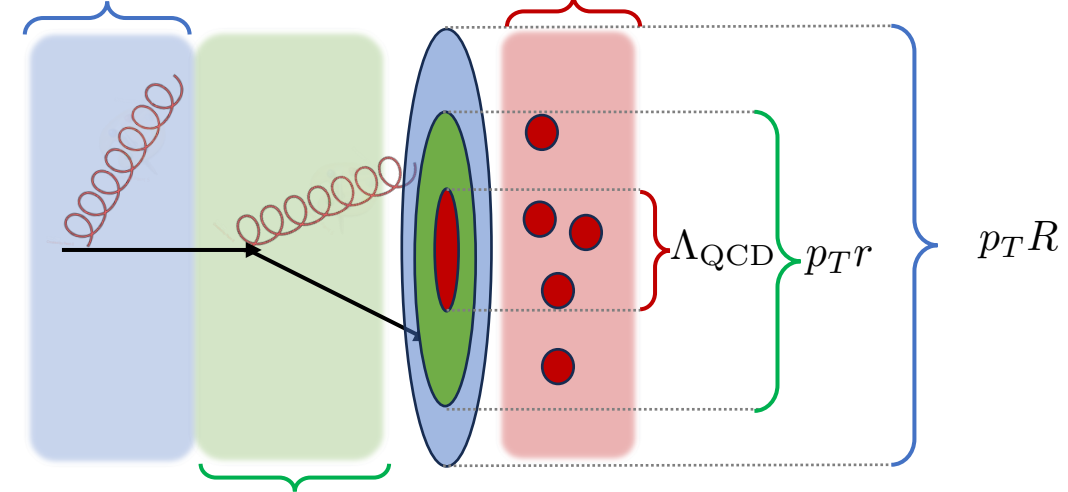
$$\psi(r, R) = \frac{\sum_{i \in j} \bar{n}_J \cdot p_i}{\sum_{i \in J} \bar{n}_J \cdot p_i}$$

$$\rho(r, R) = \frac{\partial}{\partial r} \psi(r, R)$$

Ellis, Kunszt, Soper 1992

Perturbative correction to jet direction

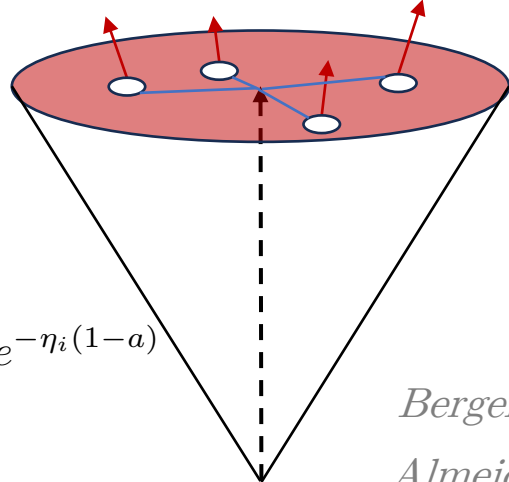
Hadronization



Perturbative correction to jet shape

IRC safety for $p_T r \gg \Lambda_{\text{QCD}}$

Jet broadening: Provides information for the width of the jet as a function of the sub-jet radius



Perturbative for $\tau_a \gg \Lambda_{\text{QCD}}/E_J$

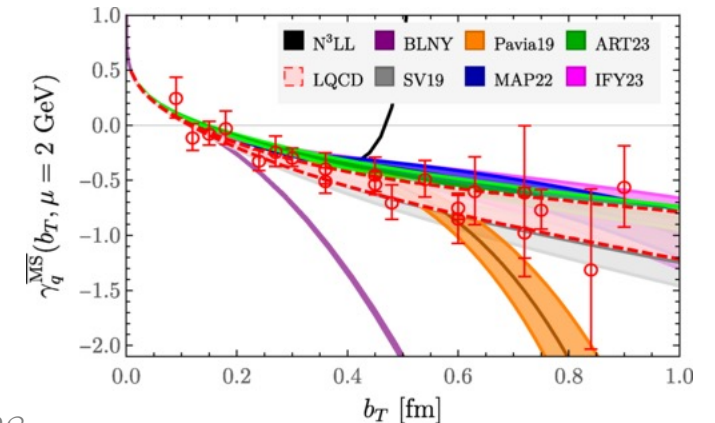
Contains some non-perturbative contributions for

$$\tau \sim \Lambda_{\text{QCD}}/E_J$$

$$\tau_a = \frac{1}{2E_J} \sum_{i \in J} |p_T^i| e^{-\eta_i(1-a)}$$

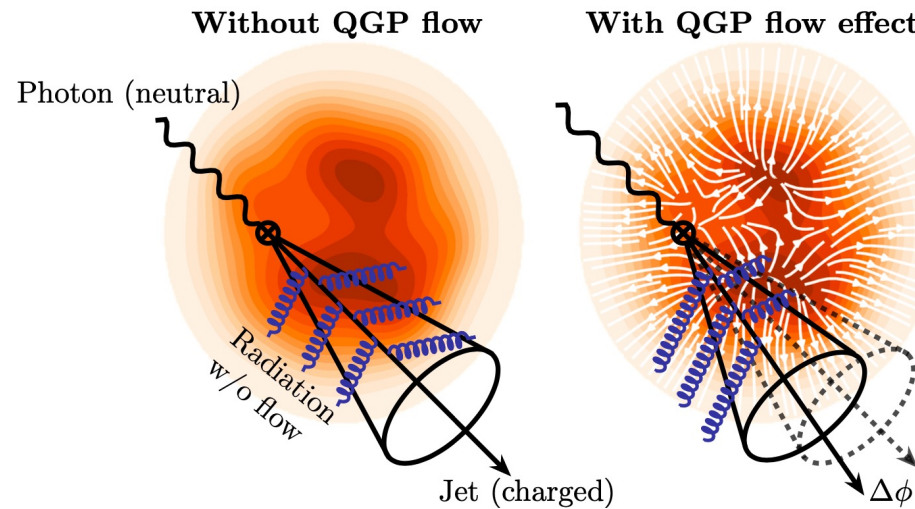
Berger, Kucs, Sterman 2003

Almeida, Lee, Perez, Sterman, Sung, Virzi 2008



Problems with jet substructure: Flowing matter

Medium-induced emissions are frequent and wide-angled. Emissions are enhanced along medium velocity



Sadofyev, Sievert, Vitev 2021

See also the talk by Joseph Bahder from week 2

Traditional jet substructure observables can tell us whether the jet is altered but they cannot tell us if it is altered more in one direction due to azimuthal integration.

$$E \frac{dN^{(1)}}{d^2k_{\perp} dx d^2p_{\perp} dE} = \frac{\alpha_s N_c}{\pi^2 x} \left(E \frac{dN^{(0)}}{d^2p_{\perp} dE} \right) \int_0^L dz \rho \int d^2q_{\perp} \bar{\sigma}(q_{\perp}^2) \times \left\{ \underbrace{\frac{2\mathbf{k}_{\perp} \cdot \mathbf{q}_{\perp}}{k_{\perp}^2 (k - q)_{\perp}^2} \left(1 - \cos \left(\frac{(k - q)_{\perp}^2}{2xE(1 - u_z)} z \right) \right)}_{\text{Isotropic emissions}} + \underbrace{\frac{q_{\perp}^2}{k_{\perp}^2 (q_{\perp}^2 + \mu^2)} \frac{\mathbf{u}_{\perp} \cdot \mathbf{k}_{\perp}}{2(1 - u_z)xE}}_{\text{Anisotropic emissions}} \right\}$$

q^{μ} Medium gluon

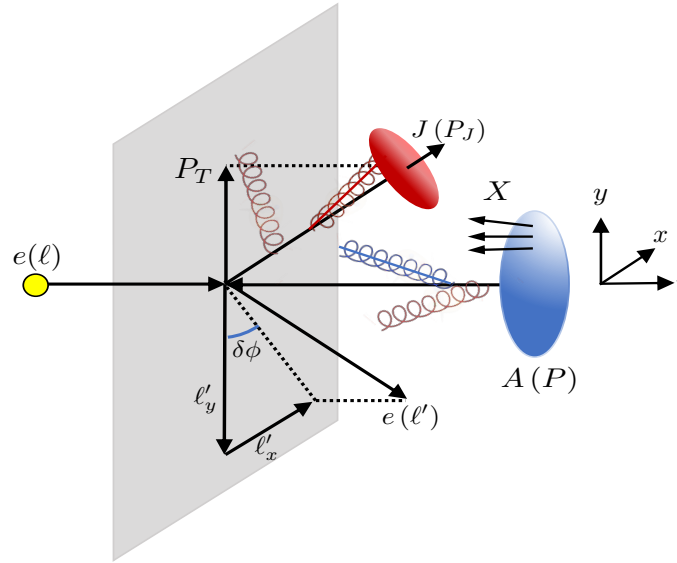
k^{μ} Stimulated emission

v^{μ} Medium velocity

Problems with jet substructure: Spin dynamics

Table of the 8 leading twist quark TMDs

N \ q	U	L	T
U	f_1		h_1^\perp
L		g_1	h_{1L}^\perp
T	f_{1T}^\perp	g_{1T}	h_{1T}^\perp h_{1T}^\perp



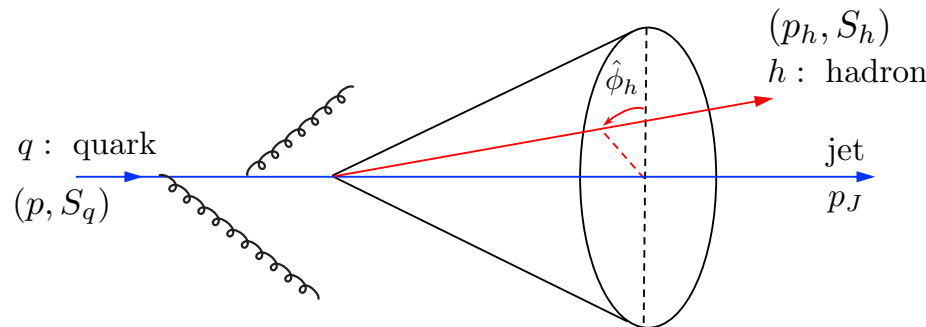
Spin information is encoded in correlations that scale like

$$J_q \sim \int d^2 q_T \left(P_{qq}(q_T) + \frac{\mathbf{q}_T \cdot \mathbf{S}}{E_J} \hat{P}_{qq}(q_T) \right)$$

Spin independent piece

Transverse spin dependence

Polarized jet fragmentation functions are excellent probes of hadronization effects, but they introduce non-perturbative content from hadronization

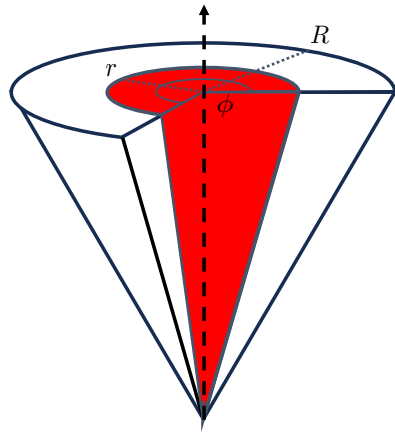


Chien, Kang, Ringer, Vitev, Xing 2015

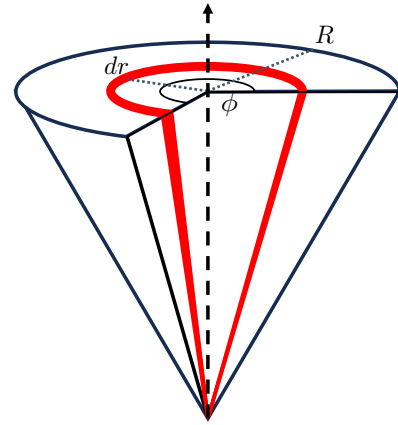
Kang, Lee, Zhao 2020

Azimuthal-dependent jet substructure

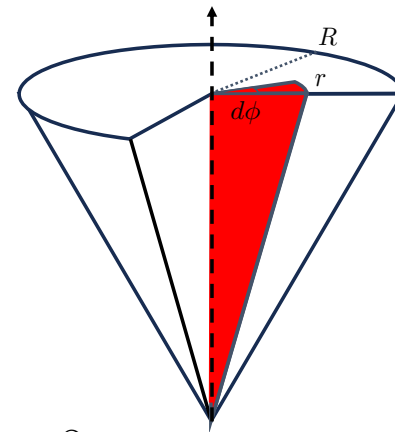
Measure the energy going into a wedge within the jet. Azimuthal-dependent jet shape



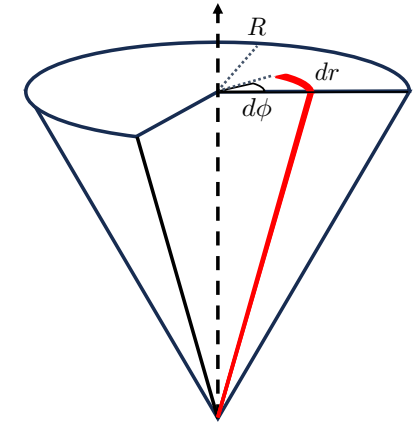
$$\psi(r, R, \varphi_i, \varphi_f)$$



$$\frac{\partial}{\partial r} \psi(r, R, \varphi_i, \varphi_f),$$

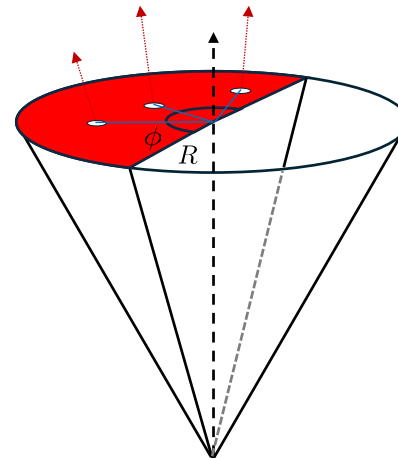


$$\frac{\partial}{\partial \varphi_f} \psi(r, R, \varphi_i, \varphi_f),$$



$$\frac{\partial}{\partial r} \frac{\partial}{\partial \varphi_f} \psi(r, R, \varphi_i, \varphi_f)$$

Measure the width of the wedge in the jet. Azimuthal-dependent jet broadening

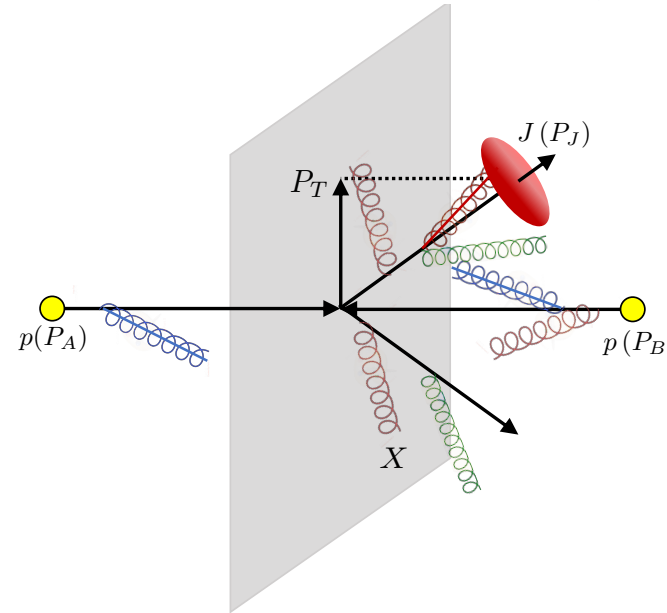
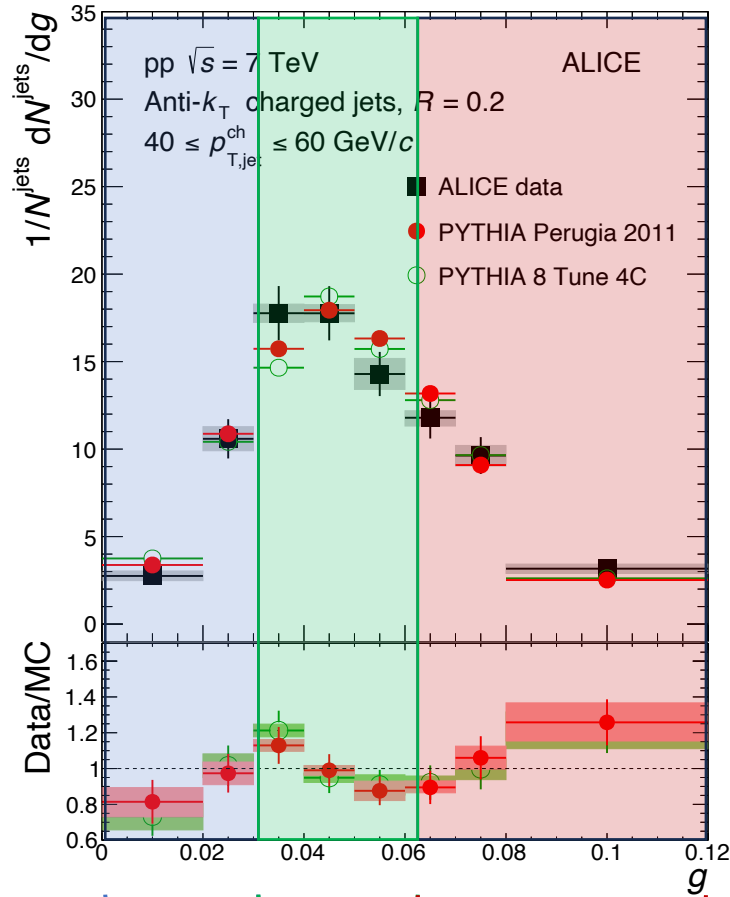


Methodology

Power counting

Jet substructure is a multi-scale problem

Cross section for single-inclusive jet production



$$d\sigma \sim H \otimes f_1 \otimes f_2 \otimes G$$

Jet substructure contained in jet function

Gluon jets take on the form

$$\hat{G}_{i \text{ alg}}^{\text{SJA}(1)}(\varphi, \tau, \omega_J, R, \mu, \zeta) = 2 \int dx d\Phi_{lq} (2\pi)^{d-1} \delta(\omega_J - \bar{n}_J \cdot l) \delta^{d-2}(\mathbf{l}_\perp) \times |\overline{\mathcal{M}}|_i^2 \Theta_{(jk) \text{ alg}}^{\text{SJA}} \delta_\tau^{\text{SJA}} \delta\left(1 - x - \frac{\bar{n} \cdot q}{\bar{n} \cdot l}\right),$$

$$G_i(z, \tau, \omega_J, R, \mu, \zeta) = H_{ij}(z, \omega_J, \mu) \int_{c-i\infty}^{c+i\infty} \frac{d\kappa}{2\pi i} \exp\left(\frac{\kappa\tau}{e^{\gamma_E}}\right) \mathcal{C}_j\left(\kappa, \omega_J, R, \mu, \frac{\zeta}{\nu^2}\right) \mathcal{S}_j(\kappa, \omega_J, R, \mu, \nu)$$

Large logs

$$N^{\text{kLL}} \sim \sum_{n=1+[k/2]}^{\infty} \alpha_s^n \ln^{2n-k}\left(\frac{\tau}{R}\right),$$

Resummed through rapidity RG

$$p_c \sim E_J(\tau^2, 1, \tau)$$

$$p_s \sim E_J \frac{\tau}{R}(R^2, 1, R)$$

Fixed order region

Soft-Collinear Effective Theory (SCET)

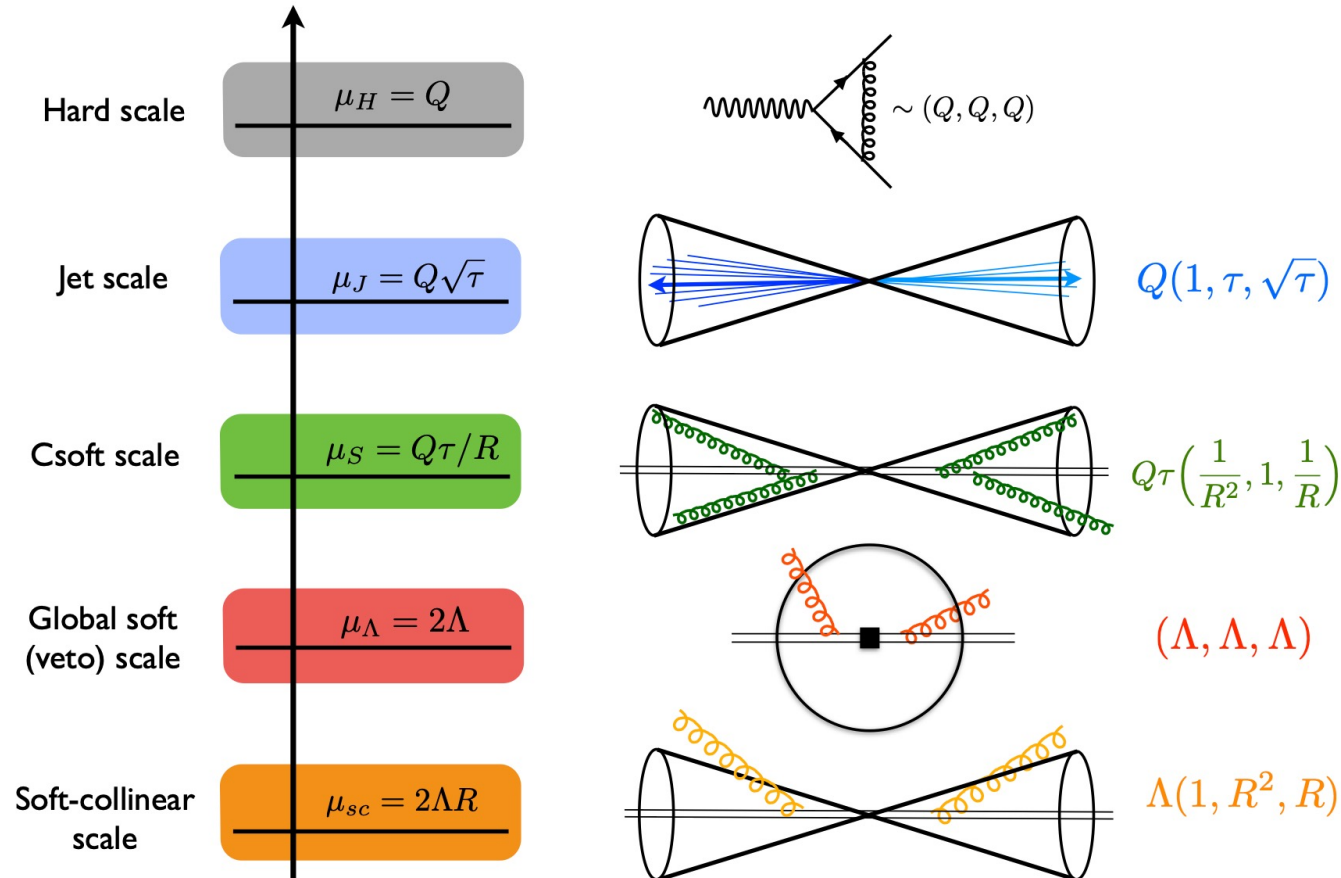
SCET is an EFT which captures soft and collinear emissions along the directions

$$\mathcal{L}_{\text{QCD}} = \sum_q \bar{\psi} i \not{D} \psi - \frac{1}{4} G_{\mu\nu}^A G^{A\mu\nu} + \mathcal{L}_{\text{gauge-fix}} + \mathcal{L}_{\text{ghost}}$$

$$\psi \rightarrow \psi_s + \psi_c \quad A^\mu \rightarrow A_s^\mu + A_c^\mu$$

$$\mathcal{L}_{\text{SCET}} = \bar{\psi}_s i \not{D}_s \psi_s - \frac{1}{4} G_{\mu\nu s}^A G_s^{A\mu\nu}$$

$$+ \xi \frac{\not{n}}{2} \left[i n \cdot D + i \not{D}_{c\perp} \frac{1}{i \bar{n} \cdot D_c} i \not{D}_{c\perp} \right] \xi - \frac{1}{4} G_{\mu\nu c}^A G_c^{A\mu\nu}$$



Bauer, Fleming, Luke 2000

Bauer, Fleming, Pirjol, Stewart 2001

Bauer, Stewart 2001

Bauer, Pirjol, Stewart 2002

Beneke, Chapovsky, Diehl, Feldmann 2002

Beneke, Feldmann 2003

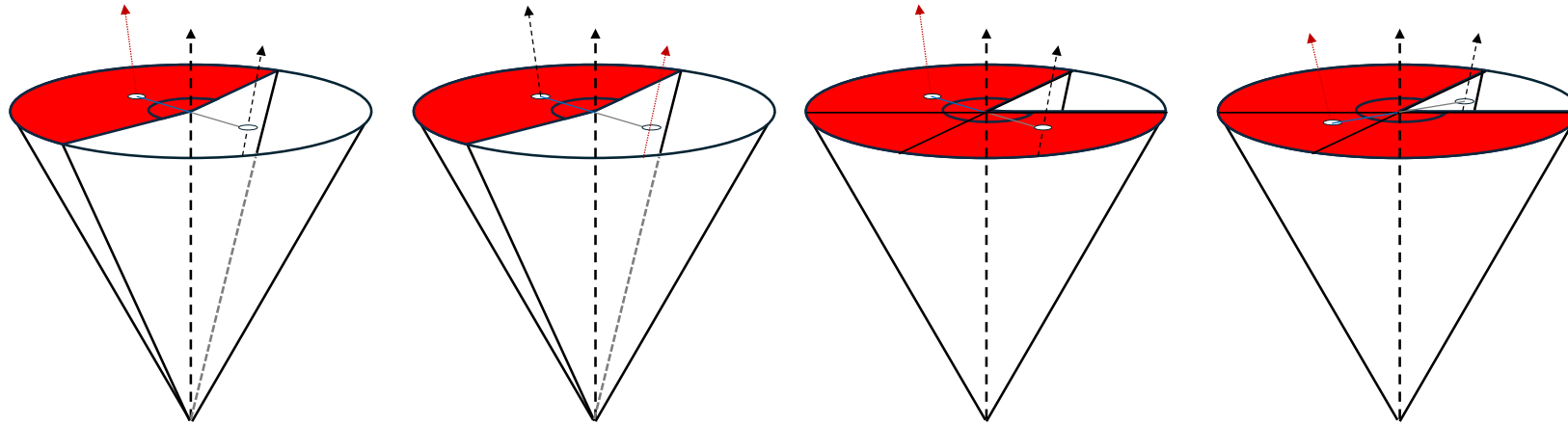
Hill, Neubert 2003

Echevarria, Idilbi, Scimemi 2011

Chien, Hornig, Lee 2015

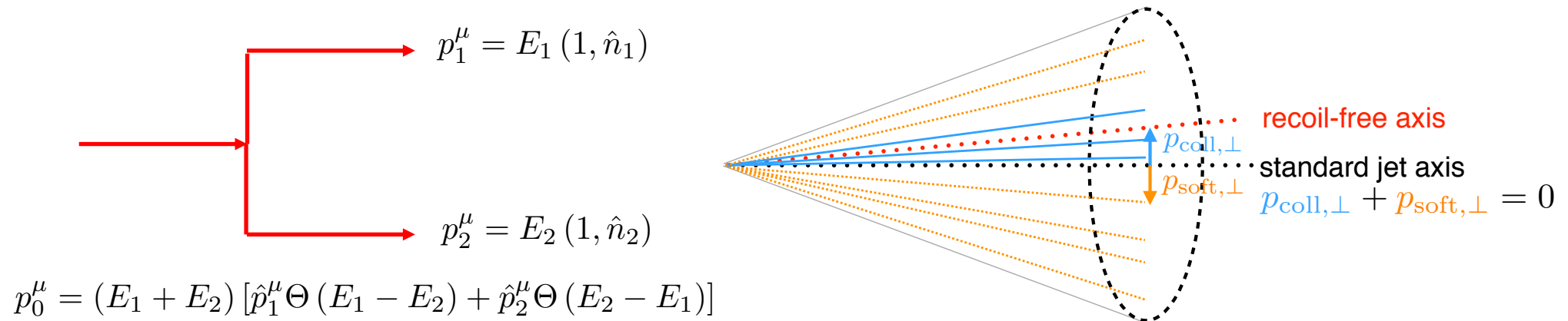
Computational details

At one loop, we have to consider permuting the different partons that enter into the jet wedge



Computation is done with both a Standard Jet Axis (SJA) with an anti- k_T algorithm and with a cone alg and a Winner Take All axis (WTA)

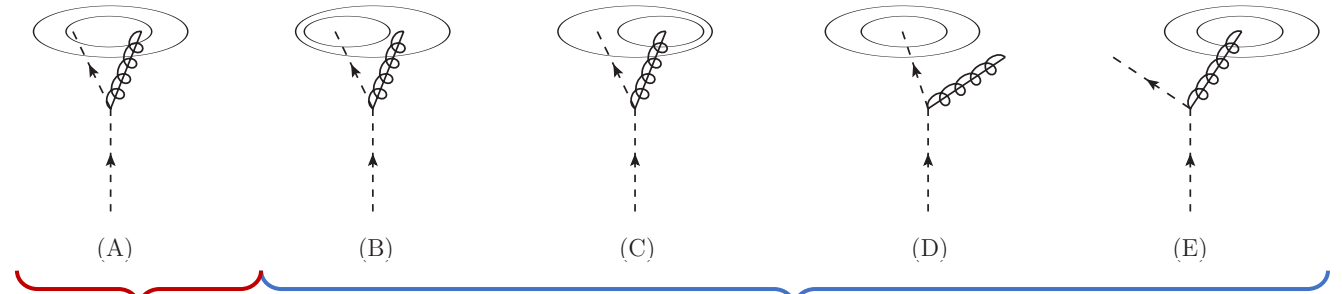
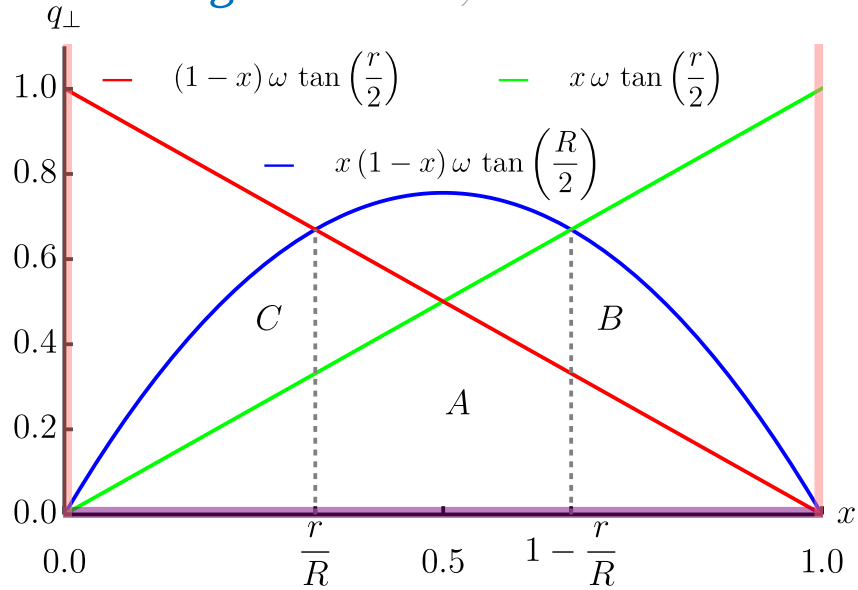
Larkoski, Neill, and Thaler (2014)



Results for the jet shape

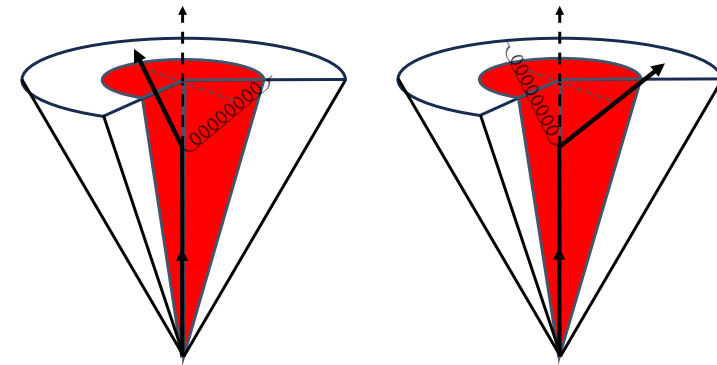
Computational details

Fixed order region Chien, Vitev 2014



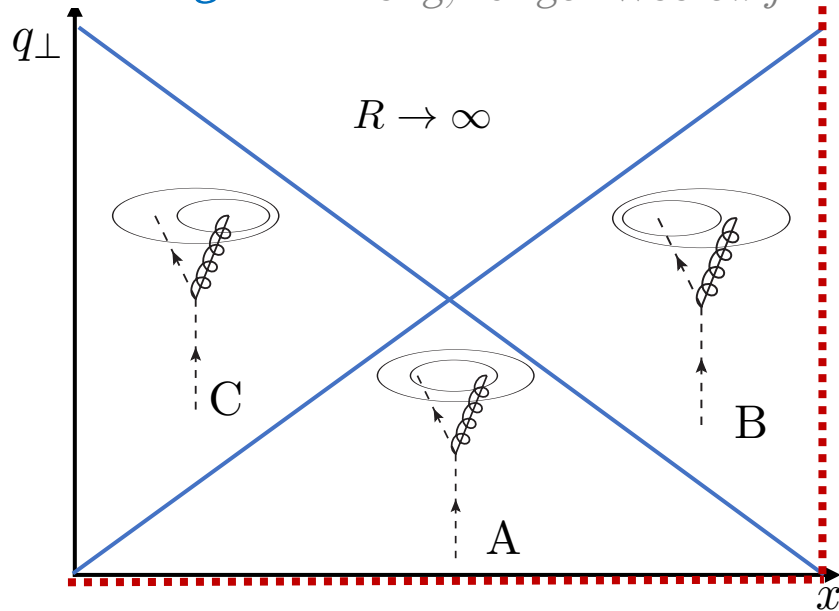
Modified in a trivially way

Undergo a non-trivial modification



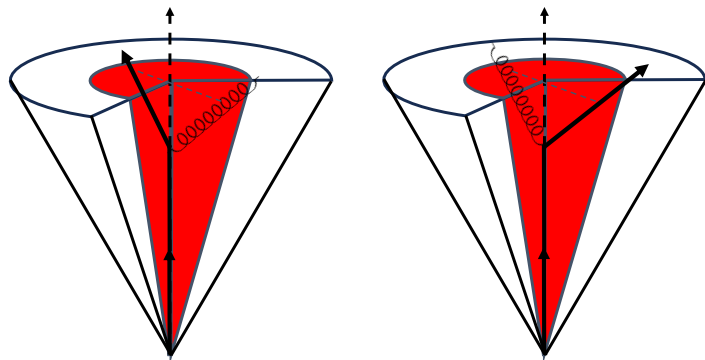
Fixed order and resummed regions are altered in the same way

Resummed region Kang, Ringer Waalewijn 2017



Consideration of IR divergences

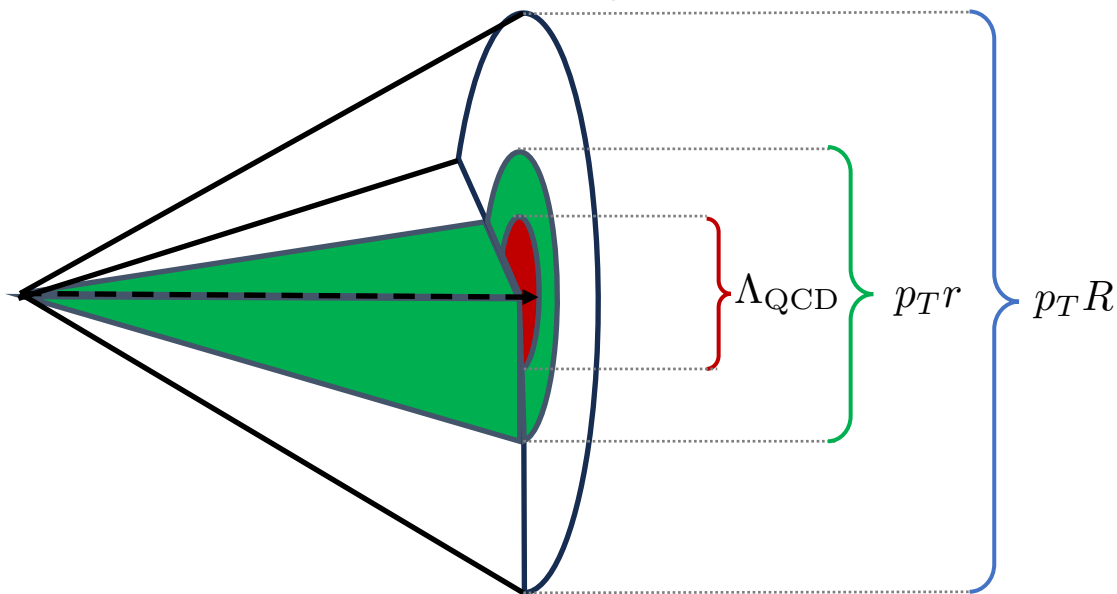
Naive computation of the jet function results in IR divergences



$$\mathcal{G}_{qkT}^{\text{SJA}(1)}(\varphi, z_w, R, \omega_J, \mu) = \frac{\alpha_s C_F}{2\pi} \left\{ \frac{\varphi}{2\pi} \left(\frac{1}{\epsilon^2} - \frac{L_R}{\epsilon} + \frac{3}{2\epsilon} + \frac{L_R^2}{2} - \frac{3}{2}L_R - \frac{17}{12}\pi^2 + 13 \right) \delta(1 - z_w) \right. \\ \left. + \left(\frac{2\pi - \varphi}{2\pi} \right) [(P_{gq}(z_w) + P_{qq}(z_w)) (L_R + 2 \ln(z_w(1 - z_w))) + 1] \right. \\ \left. + \left(\frac{2}{3}\pi^2 - \frac{13}{2} \right) \delta(1 - z_w) - \frac{1}{\epsilon_{\text{IR}}} \min\left(\frac{\varphi}{2\pi}, \frac{2\pi - \varphi}{2\pi}\right) [P_{qq}(z_w) + P_{gq}(z_w)] \right\}$$

Small kicks of transverse momentum associated with hadronization can alter the energy spectrum

Naive computation of the jet function results in IR divergences



$$\psi_{\text{alg}}^{\text{axis}}(\varphi, r, R) \sim \int dz_w z_w \mathcal{G}_{i \text{ alg}}^{\text{axis}}(\varphi, z_w, R, \omega_J, \mu)$$

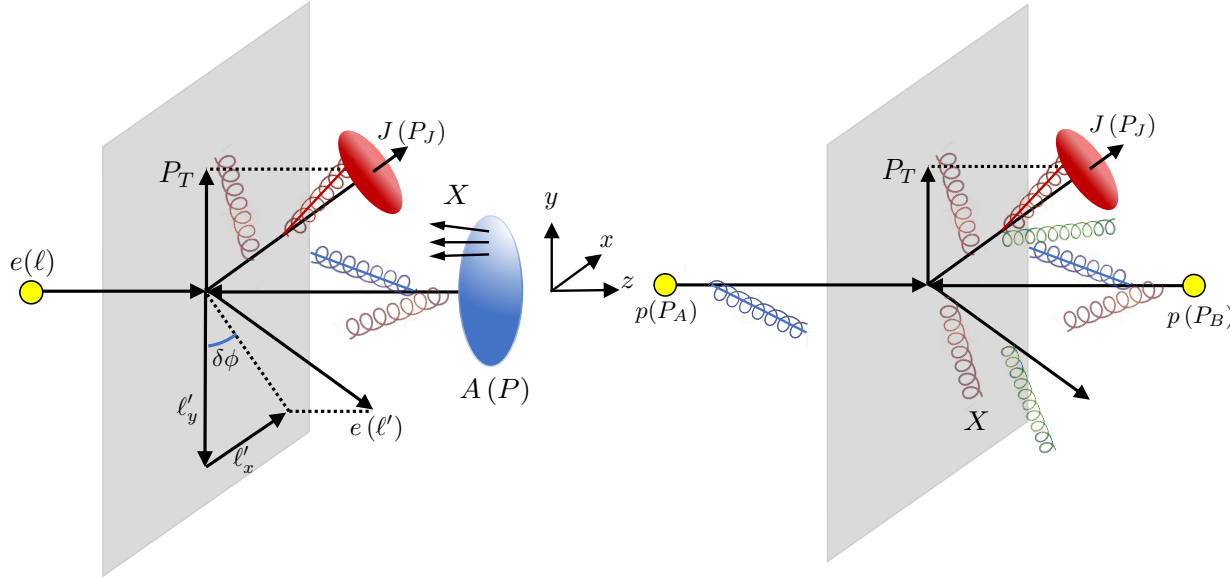
$$\frac{1}{\epsilon_{\text{IR}}} \sum_i \int dz_w z_w P_{ji}(z_w) = 0$$

The average momentum flow into and out of the wedge is zero

See for instance Moul, Zhu 2018

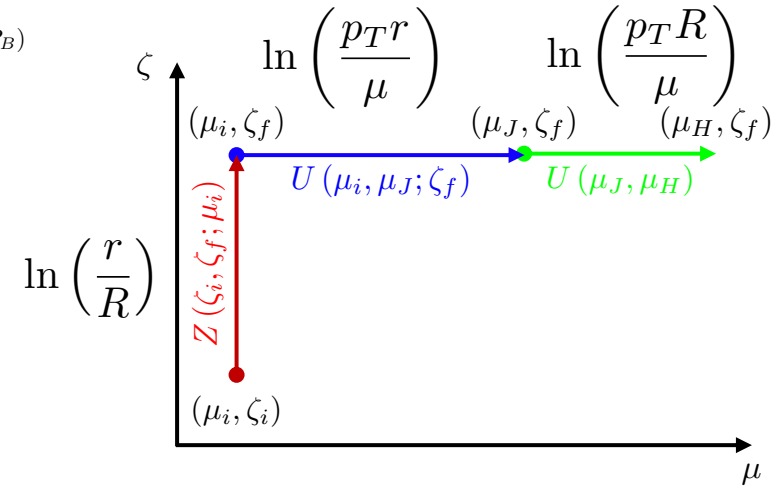
Consistency checks

To apply the jet function to multiple processes, the jet function must satisfy the evolution equation



$$\frac{d\sigma}{d\mathcal{PS}} = d\hat{\sigma} \otimes J \rightarrow \frac{d\sigma}{dz_w d\mathcal{PS}} = d\hat{\sigma} \otimes \mathcal{G}(z_w)$$

$$\frac{d\sigma}{d \ln \mu} = 0$$



The sub-jet functions obey the standard evolution equations for the exclusive and semi-inclusive jet functions

$$\frac{d}{d \ln \mu} J_{i \text{ alg}}^{\text{axis}}(p_T, R, \mu) = \frac{d}{d \ln \mu} \mathcal{G}_{i \text{ alg}}^{\text{axis}}(\varphi, z_w, p_T, R, \mu)$$

$$\frac{d}{d \ln \mu} J_{i \text{ alg}}^{\text{axis}}(z, p_T, R, \mu) = \frac{d}{d \ln \mu} \mathcal{G}_{i \text{ alg}}^{\text{axis}}(z, \varphi, z_w, p_T, R, \mu)$$

The jet shape obeys the limit

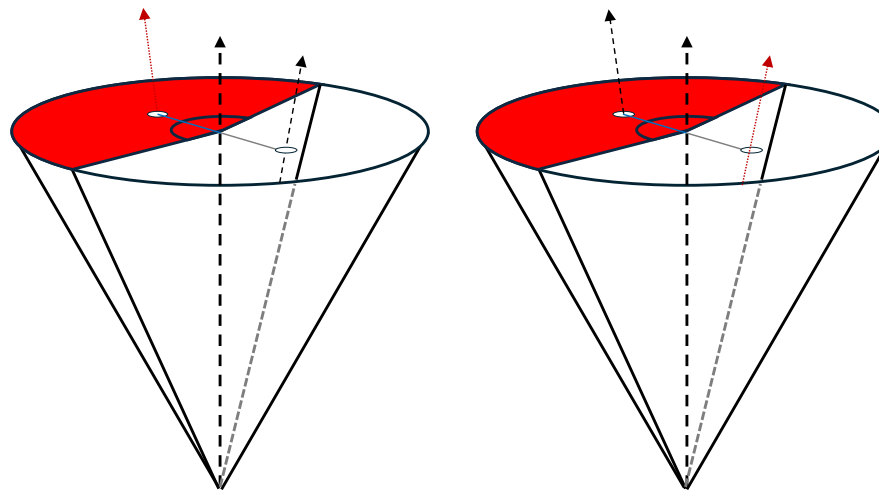
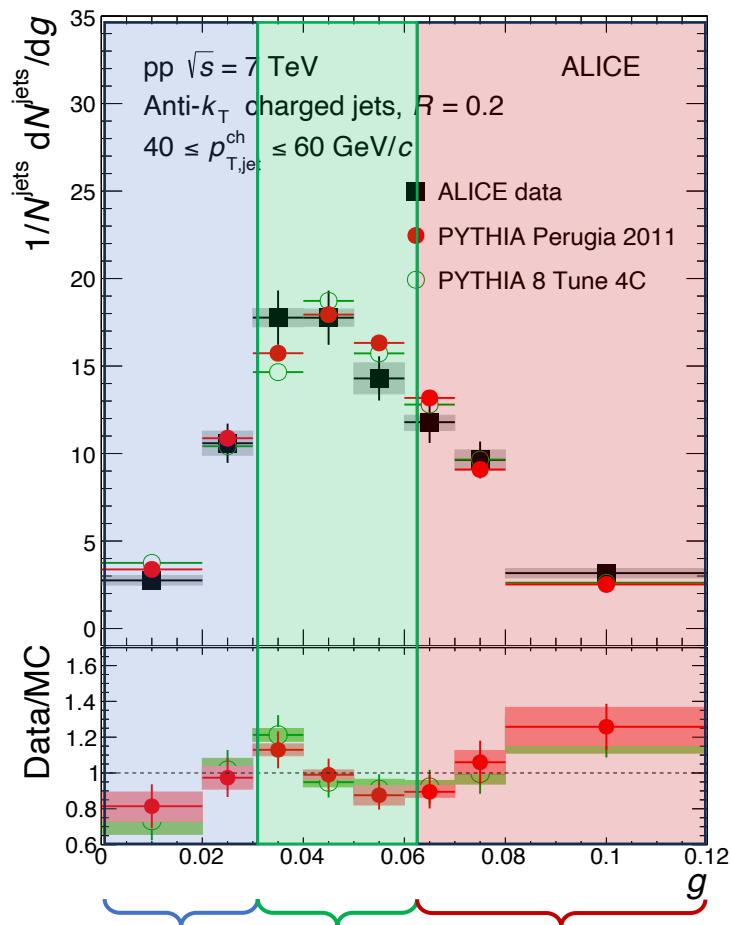
$$\lim_{\varphi \rightarrow 2\pi} \psi_{i \text{ alg}}^{\text{axis}}(\varphi, r, R) = \psi_{i \text{ alg}}^{\text{axis}}(r, R)$$

We find that this holds for all choices of axis, alg, and i

Results for the jet broadening

Azimuthal-dependent jet broadening

The computation of the jet broadening is simpler, no new non-perturbative effects



In the fixed order region, any non-perturbative effects are power suppressed

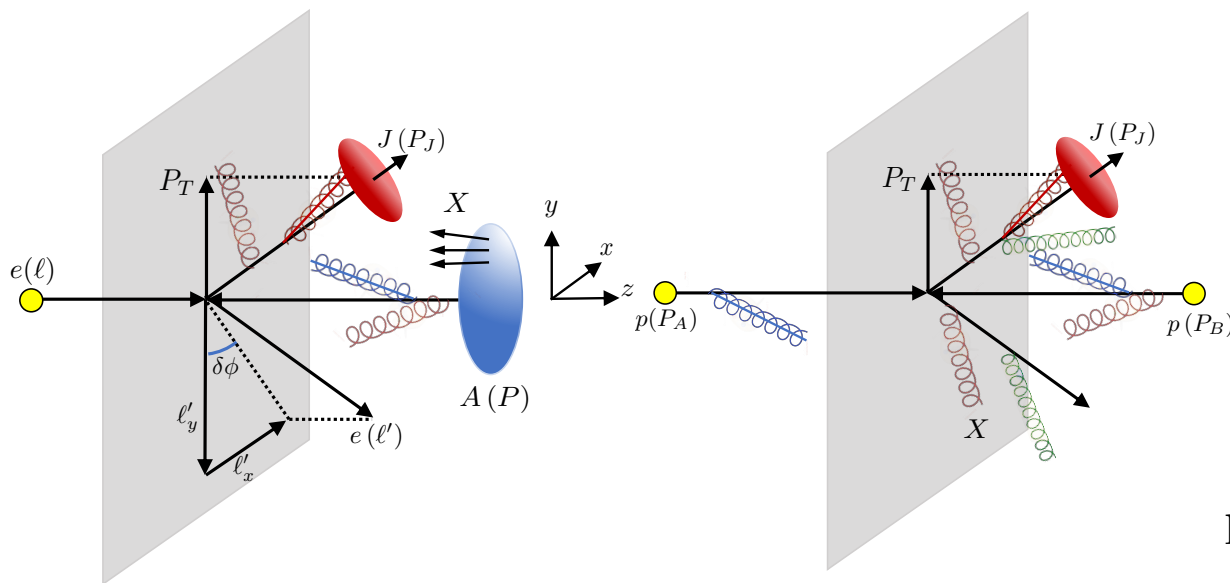
$$\tau \sim R \gg \frac{\Lambda_{\text{QCD}}}{\omega_J}$$

In the resummed region, we have contamination from the Collins-Soper effects but these are already present in the azimuthally integrated case

$$R \gg \tau \sim \Lambda_{\text{QCD}}$$

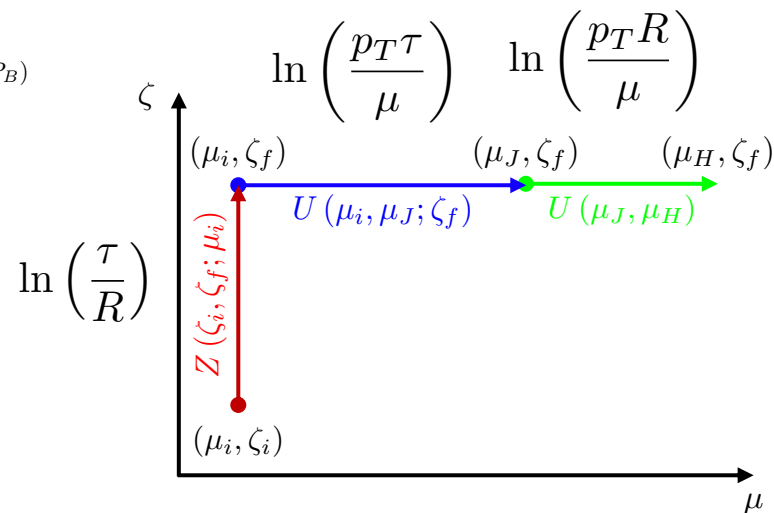
Consistency checks

To apply the jet function to multiple processes, the jet function must satisfy the evolution equation



$$\frac{d\sigma}{d\mathcal{PS}} = d\hat{\sigma} \otimes J \rightarrow \frac{d\sigma}{d\tau d\varphi d\mathcal{PS}} = d\hat{\sigma} \otimes G(\varphi, \tau)$$

$$\frac{d\sigma}{d\ln \mu} = 0$$



The sub-jet functions obey the standard evolution equations for the exclusive and semi-inclusive jet functions

$$\frac{d}{d\ln \mu} J_{i \text{ alg}}^{\text{axis}}(p_T, R, \mu) = \frac{d}{d\ln \mu} G_{i \text{ alg}}^{\text{axis}}(\varphi, \tau, p_T, R, \mu)$$

$$\frac{d}{d\ln \mu} J_{i \text{ alg}}^{\text{axis}}(z, p_T, R, \mu) = \frac{d}{d\ln \mu} G_{i \text{ alg}}^{\text{axis}}(z, \varphi, \tau, p_T, R, \mu)$$

Jet broadening functions obey the limit

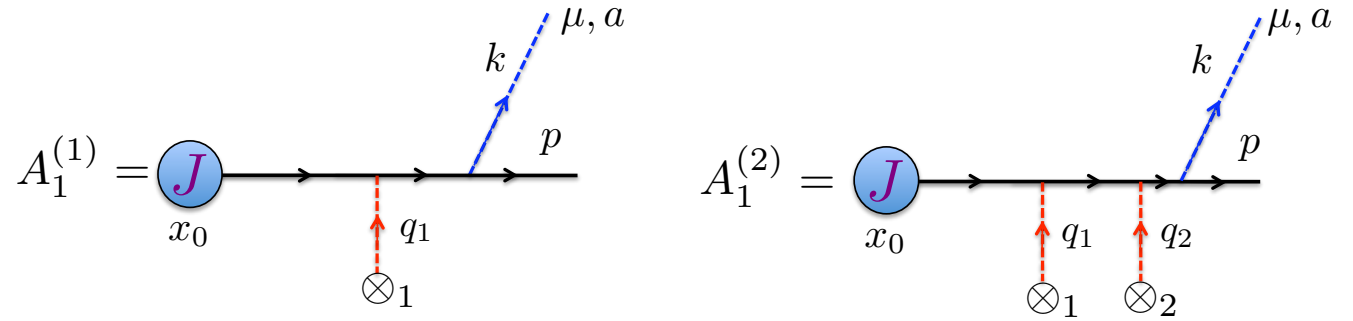
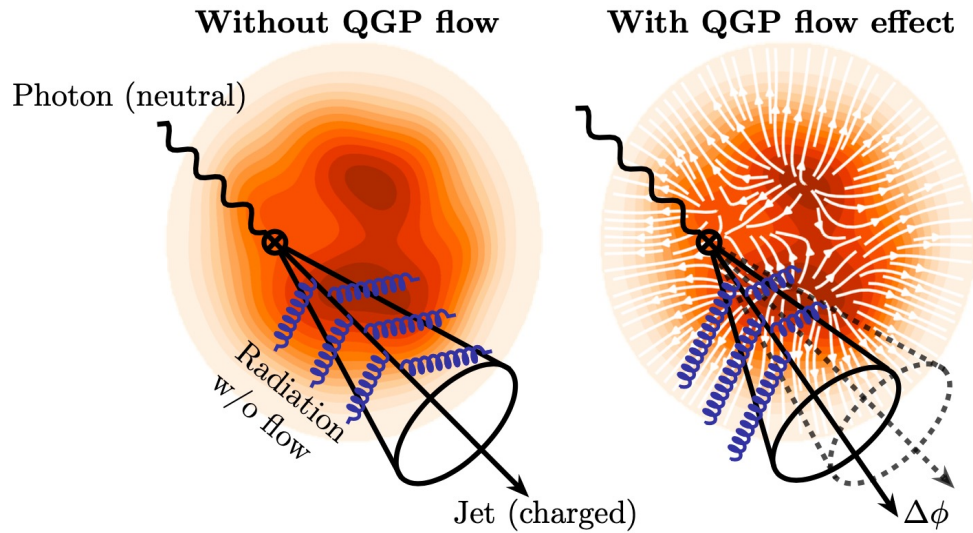
$$\lim_{\varphi \rightarrow 2\pi} G_{i \text{ alg}}^{\text{axis}}(\varphi, \tau, p_T, R, \mu) = G_{i \text{ alg}}^{\text{axis}}(\varphi, \tau, p_T, R, \mu)$$

We find that this holds for all choices of axis, alg, and i

Final words

Future work

Future work can involve computing how QGP flow can alter the jet substructure, and study which observable is an optimal probe

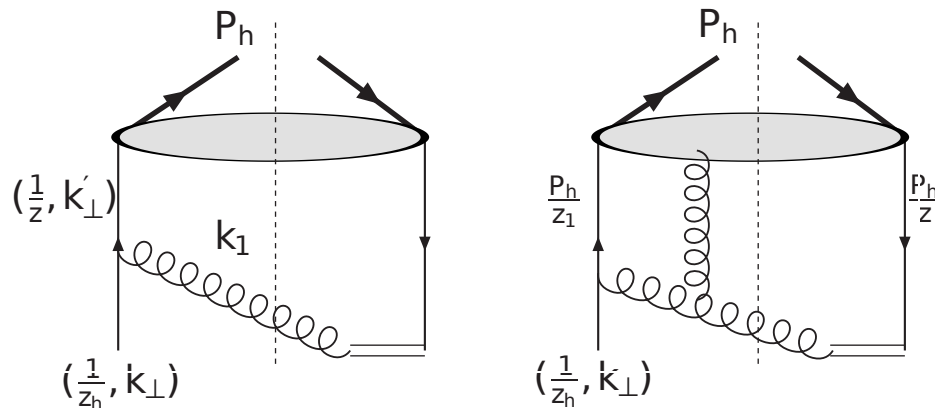


Ovanesyan, Vitev 2011

Sadofyev, Sievert, Vitev 2021

Ke, Vitev 2023

Can introduce a transverse spin to a quark, the computation associated with altering the jet substructure involves a higher twist computation.



Yuan, Zhou 2009

Conclusion

For the azimuthal integrated case, we have introduced several new results

	<i>Resummed (SJA)</i>	<i>Fixed order (SJA)</i>	<i>Resummed (WTA)</i>	<i>Fixed order (WTA)</i>
<i>Broadening</i>	<i>Becher-Bell 2012</i>	<i>Ke, Terry, Vitev 2024</i>	<i>Larkoski, Neill Thaler 2014</i>	<i>Ke, Terry, Vitev 2024</i>
<i>Jet shape</i>	<i>Kang, Ringer, Waalewijn 2017</i>	<i>Chien-Vitev 2014</i>	<i>Kang, Ringer, Waalewijn 2017</i>	<i>Kang, Ringer, Waalewijn 2017</i>

- We have introduced two azimuthal-dependent jet substructure observables*
- We have demonstrated that IR divergences enter into the new jet functions, but these are absent due to the energy weighting.*
- We have also demonstrated that the azimuthal-dependent jet broadening does not introduce any new non-perturbative contributions.*
- These new jet substructure observables have been computed in both the fixed order and resummed regions at one loop.*

Thank you to the INT

INT Research Experience for Undergraduates class of 2016



Questions?

Refactorization of the jet function in the resummation limit

The semi-inclusive jet angularity functions are given by the SCET matrix elements

$$G_q(\tau, \omega_J, R, \mu) = \frac{1}{2N_c} \text{Tr} \left[\frac{\not{n}_J}{2} \langle 0 | \delta(\omega_J - \bar{n}_J \cdot \mathcal{P}) \delta(\tau - \hat{\tau}) \chi_{n_J}(0) | J \rangle \langle J | \bar{\chi}_{n_J}(0) | 0 \rangle \right]$$

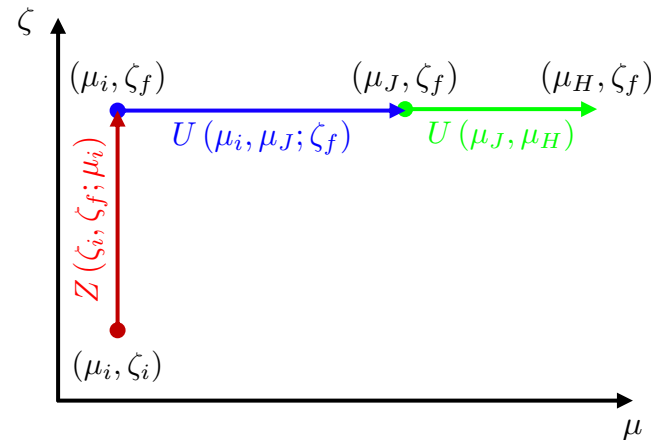
In the region where $\tau \ll R$, there are two momenta scalings which contribute to the observable

$$p_J^\mu \sim \omega_J (R^2, 1, R) \quad p_c^\mu \sim \omega_J (\lambda^2, 1, \lambda), \quad p_s^\mu \sim \omega_J \frac{\lambda}{R} (R^2, 1, R)$$

$$\mu_J \sim \omega_J R \quad \mu_c \sim \mu_s \sim \omega_J \lambda, \quad \nu_c \sim \omega_J, \quad \nu_s \sim \omega_J \frac{\lambda}{R},$$

Rapidity evolution resums logs of the power counting parameters

$$G_i(z, \tau, \omega_J, R, \mu, \zeta) = H_{ij}(z, \omega_J, \mu) \int_{c-i\infty}^{c+i\infty} \frac{d\kappa}{2\pi i} \exp\left(\frac{\kappa\tau}{e^{\gamma_E}}\right) \mathcal{C}_j\left(\kappa, \omega_J, R, \mu, \frac{\zeta}{\nu^2}\right) \mathcal{S}_j(\kappa, \omega_J, R, \mu, \nu)$$



Computation in the resummed limit

Collinear graphs for the traditional and the one-dimensional broadening

$$\tilde{C}_i^{\text{bare}} \left(\tilde{\tau}, \omega_J, \mu, \frac{\zeta}{\nu^2} \right) = \sum_j \int dx d^{d-2} q_{\perp} \hat{P}_{ji}(x, q_{\perp}) \delta \left[\tilde{\tau} - \frac{2q_{\perp}}{\omega_J} \right] \left(\frac{\nu^2}{(1-x)^2 \zeta} \right)^{\eta/2}$$

$$C_i^{\text{bare}} \left(\tau, \omega_J, \mu, \frac{\zeta}{\nu^2} \right) = \sum_j \int dx d^{d-2} q_{\perp} \hat{P}_{ji}(x, q_{\perp}) \delta \left[\tau - \frac{2q_x}{\omega_J} \right] \left(\frac{\nu^2}{(1-x)^2 \zeta} \right)^{\eta/2}$$

Soft graphs for the traditional and the one-dimensional broadening

$$\begin{aligned} \tilde{S}_i^{\text{bare}}(\tilde{\tau}, \omega_J, R, \mu, \nu) &= g^2 C_i \left(\frac{\mu^2 e^{\gamma_E}}{4\pi} \right)^{\epsilon} \int \frac{dl_J^+ dl_J^- d^{d-2} l_{\perp}}{(2\pi)^d} \frac{n_J \cdot \bar{n}_J}{n_J \cdot l \bar{n}_J \cdot l} 2\pi \delta(l^2) \\ &\quad \times \delta \left(\tilde{\tau} - 2 \frac{l_{\perp}}{\omega_J} \right) \Theta \left(\tan^2 \frac{R}{2} - \frac{l^+}{l^-} \right) \left(\frac{2l_0}{\nu} \right)^{\eta} \end{aligned}$$

$$\begin{aligned} S_i^{\text{bare}}(\tau, \omega_J, R, \mu, \nu) &= g^2 C_i \left(\frac{\mu^2 e^{\gamma_E}}{4\pi} \right)^{\epsilon} \int \frac{dl_J^+ dl_J^- dl_x d^{d-3} l_{\perp}}{(2\pi)^d} 2\pi \delta(l^2) \frac{n_J \cdot \bar{n}_J}{n_J \cdot l \bar{n}_J \cdot l} \\ &\quad \times \delta \left(\tau - 2 \frac{l_x}{\omega_J} \right) \Theta \left(\tan^2 \frac{R}{2} - \frac{l^+}{l^-} \right) \left(\frac{2l_0}{\nu} \right)^{\eta} \end{aligned}$$

Requires additional integration in d-3 dimensions

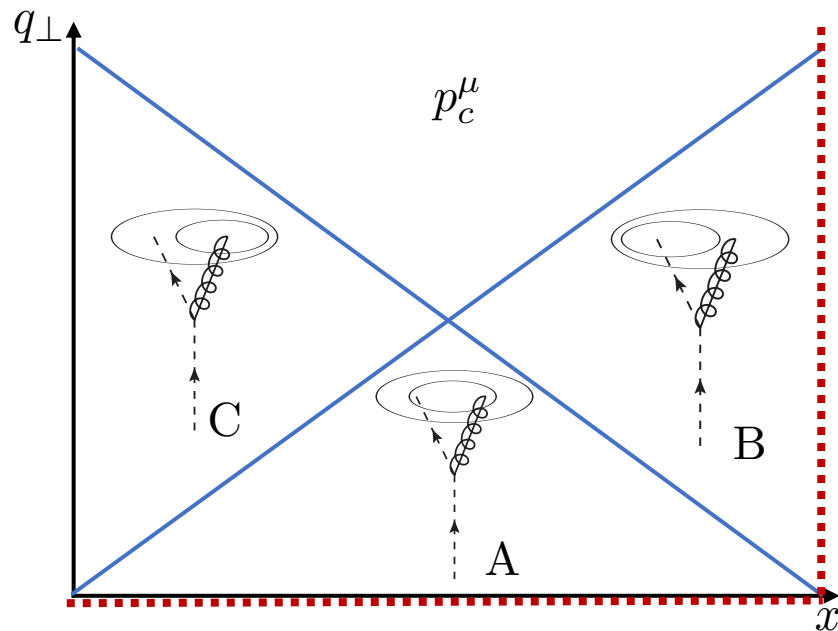
Fixed order computation

The semi-inclusive jet angularity functions are given by the SCET matrix elements

$$G_q(\tau, \omega_J, R, \mu) = \frac{1}{2N_c} \text{Tr} \left[\frac{\vec{n}_J}{2} \langle 0 | \delta(\omega_J - \vec{n}_J \cdot \mathcal{P}) \delta(\tau - \hat{\tau}) \chi_{n_J}(0) | J \rangle \langle J | \bar{\chi}_{n_J}(0) | 0 \rangle \right]$$

Power counting and refactorization

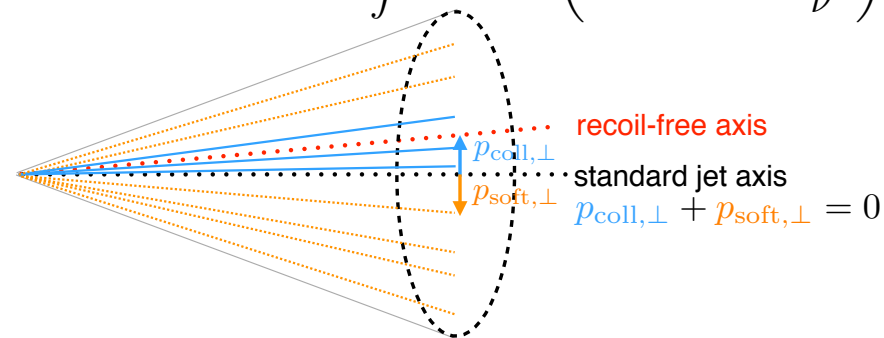
In the region where $r \ll R$, the jet algorithm no longer regulates the rapidity divergences (SCET II). There are three modes that contribute to the observable



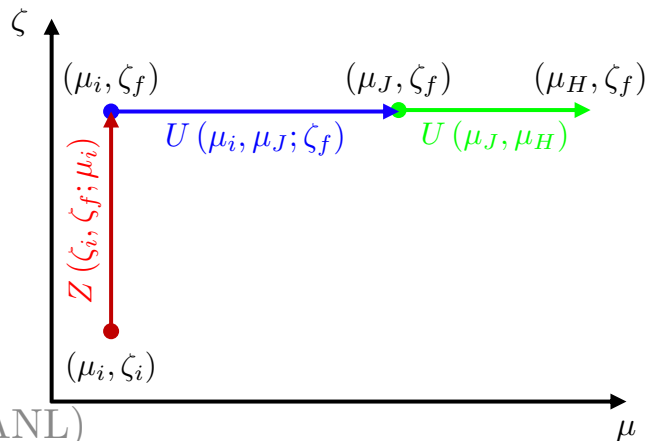
$$p_J^\mu \sim \omega_J (R^2, 1, R) \quad p_c^\mu \sim \omega_J (r^2, 1, r) \quad p_s^\mu \sim \omega_J \frac{r}{R} (R^2, 1, R)$$

$$\mu_J \sim \omega_J R \quad \mu_c \sim \mu_s \sim \omega_J r \quad \nu_s \sim \omega_J \frac{r}{R} \quad \nu_c \sim \omega_J$$

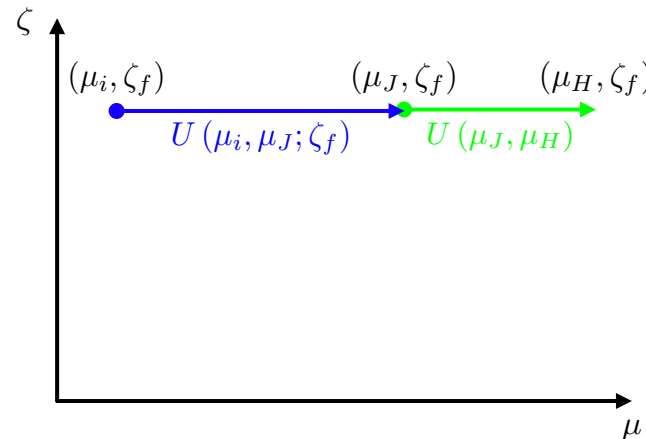
$$j_c(z, z_r, \omega_J, r, R, \mu) = H_{cd}(z, \omega_J, \mu) \int d^2 k_\perp C_d\left(z_r, k_\perp, \omega_j, \mu, \frac{\zeta}{\nu^2}\right) S_d(k_\perp, R, \omega_j, \mu, \nu)$$



Evolution occurs in three parts

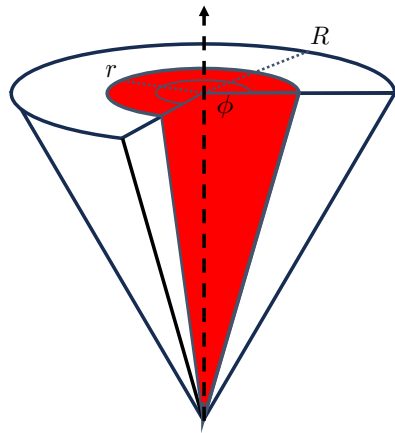


Recoil issue can be removed using a WTA axis

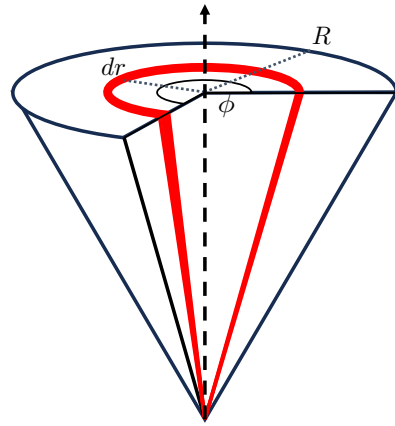


The azimuthal dependent jet shape

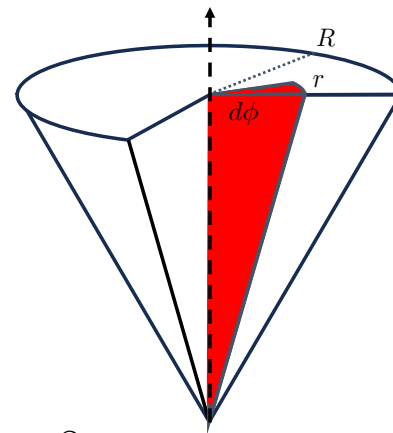
We generalize the jet shape to also contain azimuthal angle dependence



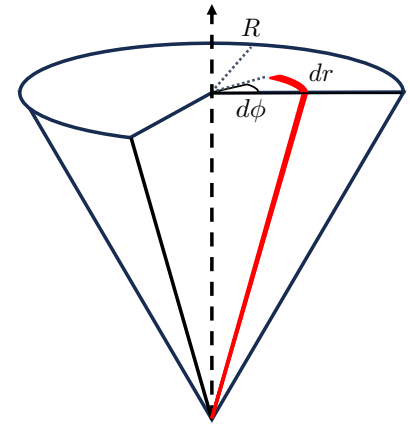
$$\psi(r, R, \varphi_i, \varphi_f)$$



$$\frac{\partial}{\partial r} \psi(r, R, \varphi_i, \varphi_f),$$



$$\frac{\partial}{\partial \varphi_f} \psi(r, R, \varphi_i, \varphi_f),$$



$$\frac{\partial}{\partial r} \frac{\partial}{\partial \varphi_f} \psi(r, R, \varphi_i, \varphi_f)$$

Factorization is unchanged but the ingredients are modified

$$j_c(z, z_r, \varphi_i, \varphi_f, \omega_J, r, R, \mu) = H_{cd}(z, \omega_J, \mu) \int d^2 k_\perp C_d\left(z_r, \mathbf{k}_\perp, \varphi_i, \varphi_f, \omega_j, \mu, \frac{\zeta}{\nu^2}\right) S_d(\mathbf{k}_\perp, R, \mu, \nu)$$

Same as integrated at NLO

Tree level modified trivially

Same as integrated at NLO

Non-trivial NLO modification

Anomalous dimension of jet shape unchanged